

Translational Relevance

A wide variety of biomarkers of antiangiogenic inhibitors have been proposed and intensively investigated; however, no biomarkers have been validated for routine clinical use and a new pharmacodynamic biomarker is needed. We have shown in this study that (i) BIBF 1120, a VEGF receptor 2 (VEGFR2) inhibitor, exhibited potent antitumor and antiangiogenic activity against hepatocellular carcinoma *in vivo* and (ii) VEGFR2⁺pTyr⁺ peripheral blood leukocytes (PBL) were useful pharmacodynamic biomarker *in vivo*. Our findings indicate the clinical utility of VEGFR2⁺pTyr⁺ PBLs as a feasible, noninvasive, and VEGF signal-specific biomarker of VEGFR2 tyrosine kinase inhibitors for use in early clinical trials.

antiangiogenic drugs for evaluating their effects (12, 13). Indeed, we have shown that soluble VEGFR2 was certainly decreased by BIBF 1120 treatment in a phase I trial; however, this decrease was observed at a relatively late stage, 8 to 29 days after the start of treatment (14). These results suggest that soluble VEGFR2 is not a rapid-responding biomarker for monitoring effects of antiangiogenic drugs. As no other biomarkers have been validated for routine clinical use, a new pharmacodynamic biomarker is needed.

BIBF 1120 is a potent triple angiokinase inhibitor that inhibits VEGFR1, 2, and 3, fibroblast growth factor receptors (FGFR), and platelet-derived growth factor receptors (PDGFR). *In vitro* studies have shown that VEGFR2 tyrosine kinase activity was potently inhibited by BIBF 1120 ($IC_{50} = 21$ nmol/L) and was also active against VEGFR1 and 3 ($IC_{50} = 34$ and 13 nmol/L, respectively; ref. 15). BIBF 1120 dose dependently inhibited the growth of various human tumor xenografts and tumor angiogenesis *in vivo* studies, consistent with the potent inhibition of VEGF signaling (15). BIBF 1120 also exhibited a relatively strong direct growth inhibitory effect on cancer cell lines, influencing 9 of 14 acute myeloid leukemia cell lines in a colony formation assay with an IC_{50} value of less than 1 μ mol/L (16).

We previously reported the antitumor activity of VEGFR2 tyrosine kinase inhibitors (TKI) against non-small cell lung cancer and gastric cancer, identifying a biomarker and the mode of action (17–19). In the present study, we focused on the antitumor activity of BIBF 1120 against HCC, which is hypervascular in nature. In addition, to identify a pharmacodynamic biomarker, we examined the phosphorylation levels of VEGFR-positive peripheral blood leukocytes (PBL) as a surrogate tissue in an *in vivo* model.

Materials and Methods

Compounds

BIBF 1120 was provided by Boehringer Ingelheim Pharma GmbH & KG. 5-Fluorouracil (5FU; Sigma-Aldrich) and an epidermal growth factor receptor (EGFR) TKI,

AG1478 (Biomol International), were purchased from the indicated companies.

Cell lines and cultures

HepG2, HLF, HLE, and Huh7 (human hepatoblastoma and HCC cell lines, respectively) were maintained in Dulbecco's modified Eagle's medium supplemented with 10% FBS (Gibco BRL). HUVECs (human umbilical vein endothelial cells) were purchased from Kurabo and were maintained in Hmedia-EG2 (Kurabo) medium with 2% FBS, 2 ng/mL of VEGF-A (R&D Systems), 10 ng/mL of EGF, 5 ng/mL of FGF, 10 μ g/mL of heparin, and 1 μ g/mL of cortisol. These cells were cultured in an atmosphere of 5% CO_2 at 37°C.

In vitro growth inhibition assay

The growth inhibitory effects of BIBF 1120 on the HepG2, HLF, HLE, and Huh7 cell lines were examined using an MTT assay as previously described (17, 18). The optical density was measured at 570 nm. Three independent experiments were conducted.

Western blot analysis

The antibodies used for the Western blot analysis were anti-KDR (IBL), anti-phospho (p)-VEGFR2 (Tyr1175), anti-VEGFR1, anti-p44/42 MAPK (mitogen-activated protein kinase), anti-p-p44/42 MAPK, anti-c-Kit, anti-PDGFR β , anti-FGFR1, 2, and 3, horseradish peroxidase-conjugated secondary antibody (Cell Signaling Technology), and anti- β -actin (Santa Cruz Biotechnology). The methods have been previously described (18). Two independent immunoblotting experiments were conducted.

Tube formation assay

HUVECs were cultured without VEGF-A for 24 hours. A total of 40 μ L of Matrigel (BD Bioscience) and 20 μ L of PBS were mixed and incubated in 96-well plates. After the gel had solidified, a 100- μ L volume of HUVECs (2×10^4 cells/well) was seeded onto the plates with 20 ng/mL of VEGF-A and the indicated concentration of BIBF 1120. The 96-well plates were then incubated for 4 hours. Capillary morphogenesis was evaluated under a microscope (Olympus). This assay was carried out in 3 independent experiments.

Real-time reverse transcriptase PCR

The method has been previously described (17). The primers used for real-time reverse transcriptase PCR (RT-PCR) are shown in Supplementary Table 1. GAPD was used to normalize the expression levels in the subsequent quantitative analyses.

Flow cytometric analysis for HUVECs

HUVECs were seeded on 6-well plates without VEGF-A for 24 hours. After exposure to BIBF 1120, AG1478, or 5FU for 3 hours, the cells were stimulated with 20 ng/mL of VEGF-A for 30 minutes. The flow cytometric procedure was carried out according to the manufacturer's protocols,

using the Fixation/Permeabilization Kit (BD Biosciences); the data were obtained using a FACS Calibur flow cytometer (BD Biosciences). Anti-phosphotyrosine (pTyr) antibody (P-Tyr-100; Cell Signaling) was used to detect the phosphorylation levels.

Flow cytometric analysis for PBLs in the *in vivo* model

In the *in vivo* model, about 0.5 to 1 mL of peripheral blood was obtained from treated mice and 20 ng/mL of VEGF was added to the whole blood samples for 20 minutes. The red cells were then lysed using a lysis buffer (155 mmol/L NH₄Cl, 10 mmol/L NaHCO₃, and 1 mmol/L EDTA2Na, pH 7.3) for 10 minutes, and leukocytes were fixed and permeabilized using a Fixation/Permeabilization Kit for analysis. The following antibodies were used: anti-mouse CD45-PerCP, anti-mouse Flk-1-PE (BD Biosciences), anti-pTyr (P-Tyr-100; Cell Signaling), and Alexa Fluor Mouse IgG1 Isotype Control (BD Pharmingen). The analysis was carried out using the WinMDI software (20).

HCC xenograft model

Nude mice (BALB/c nu/nu; 6-wk-old females; CLEA Japan Inc.) were used for the *in vivo* studies and were cared for in accordance with the recommendations for the handling of laboratory animals for biomedical research, compiled by the Committee on Safety and Ethical Handling Regulations for Laboratory Animal Experiments, Kinki University. The ethical procedures followed and met the requirements of the United Kingdom Coordinating Committee on Cancer Research Guidelines.

Mice were subcutaneously inoculated with a total of 6×10^6 HepG2 cells. Two weeks after inoculation, the mice were randomized according to tumor size into 3 groups to equalize the mean pretreatment tumor size among the 3 groups ($n = 6$ in each group). The mice were then treated with BIBF 1120 (50 mg/kg/d, p.o.), BIBF 1120 (100 mg/kg/d, p.o.), or the vehicle control (saline, p.o.) for 14 days (Fig. 3A–C). On day 14, the mice were euthanized, blood samples were collected by cardiac puncture, and tumor specimens were collected for immunohistochemistry. The tumor volume was calculated as the length \times width² \times 0.5 and was assessed every 2 to 3 days.

Immunohistochemical analysis

A mouse anti-CD31 monoclonal antibody (1:100; BD Biosciences) was used to detect the endothelial cells. The paraffin-embedded samples were cut into 4- μ m sections, deparaffinized, and placed in a preheated antigen retrieval solution (Dako) in a steamer for 10 minutes. All the samples were then blocked in 3% H₂O₂ in methanol for 15 minutes and rinsed with PBS. The slides were then placed in a Sequenza slide staining system (Thermo Fisher Scientific) and blocked in 1% normal goat serum for 20 minutes. The slides were incubated overnight at 4°C with the CD31 antibody. A standard avidin-biotin peroxidase complex assay was then carried out using the ABC Elite Kit (Vector Laboratories). The slides were developed with 3,3'-diaminobenzidine (DAB; Zymed Laboratories) and coun-

terstained with 10% hematoxylin. Microvessel density (MVD) was quantified by measuring the number of CD31-positive endothelial cells in the tumors. Ten random fields per tumor sample at 200 \times magnification were captured and saved for computer-assisted image analysis using the ImageJ software package (21). An algorithm for color deconvolution was used to segregate the brown DAB-positive CD31 endothelial cells and the blue tumor cells. Thresholds were adjusted to remove background and non-specific signals. MVD was reported as the average ratio of CD31-positive cells to tumor cells.

Statistical analysis

The statistical analyses were carried out using Microsoft Excel (Microsoft) to calculate the SD and to test for statistically significant differences between the samples using a Student's *t* test. A value of $P < 0.05$ was considered statistically significant.

Results

BIBF 1120 potently inhibits VEGFR2 signaling in HUVECs

We evaluated the inhibitory effect of BIBF 1120 at various concentrations (0.0001–10 μ mol/L) on VEGFR2 signaling, using HUVECs stimulated with 20 ng/mL of VEGF. BIBF 1120 at a concentration of 0.01 μ mol/L completely inhibited the phosphorylation of VEGFR2 and MAPK in HUVECs (Fig. 1A). BIBF 1120 at a concentration of 0.01 μ mol/L partially inhibited tube formation in HUVECs stimulated with VEGF, whereas BIBF 1120 at a concentration of 1 μ mol/L completely inhibited tube formation (Fig. 1B). These data indicate that BIBF 1120 potently inhibits VEGFR2 signaling in endothelial cells.

Flow cytometry detects BIBF 1120-induced inhibition of pTyr levels

To detect the BIBF 1120-induced inhibition of pTyr levels by flow cytometry, the VEGF-induced pTyr levels of proteins in HUVECs were evaluated after exposure to BIBF 1120, the EGFR TKI AG1478 as a TKI control, or 5FU as a cytotoxic drug control. The controls agents were used to show that another target of TKI did not induce (AG1478) or to exclude the possibility that nonspecific effects such as cytotoxic cellular responses were not induced (5FU). Flow cytometry revealed that the VEGF-induced pTyr levels in HUVECs were significantly inhibited by BIBF 1120 at concentration of 1 and 5 μ mol/L but not by AG1478 or by 5FU (Fig. 1C and D). This flow cytometric method is considered a feasible means of detecting the inhibition of VEGF-induced pTyr levels induced by VEGFR2 TKIs.

Growth inhibitory effects and expression status of targeted receptors in HCC cell lines *in vitro*

To evaluate the expression status of the putative targeted receptors of BIBF 1120 in the 4 HCC cell lines and HUVECs as a control, we examined the protein expression levels of VEGFR1, VEGFR2, FGFR1, FGFR2, FGFR3, PDGFR β , and

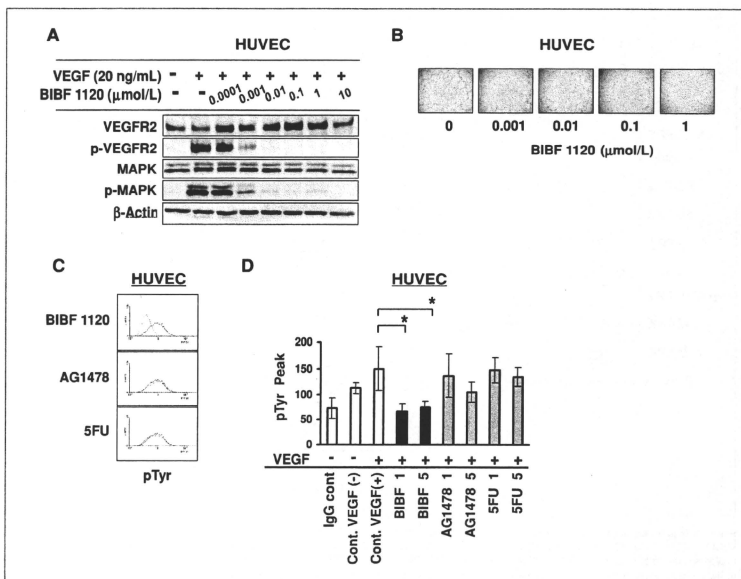


Figure 1. Inhibition of VEGFR2 signaling by BIBF 1120 and detection of the inhibition of pTyr by flow cytometry in HUVECs. **A**, the inhibition of VEGFR2 and MAPK phosphorylation by BIBF 1120 was determined using a Western blot analysis. HUVECs cultured in a medium containing 2% FBS were exposed to BIBF 1120 (0.0001–10 μmol/L) for 3 hours, stimulated with 20 ng/mL of VEGF for 15 minutes, and lysed for analysis. **B**, effect of BIBF 1120 on the inhibition of tube formation. HUVECs were seeded with 20 ng/mL of VEGF-A and exposed to BIBF 1120 (0.001–1 μmol/L) on Matrigel-layered 96-well plates for 4 hours. Capillary morphogenesis was evaluated under a microscope. This assay was conducted in 3 independent experiments. **C** and **D**, HUVECs were seeded on 6-well plates without VEGF-A for 24 hours. After exposure to BIBF 1120, AG1478, or 5FU for 3 hours, the cells were stimulated with 20 ng/mL of VEGF-A for 30 minutes. The inhibition of pTyr level was detected by flow cytometry with an anti-pTyr antibody. Note that only BIBF 1120 significantly inhibited the VEGF-induced phosphorylation levels of tyrosine. This assay was conducted in 3 independent experiments; bars, SD. *, $P < 0.05$.

c-Kit (the kinase activities of which are reportedly inhibited by BIBF 1120 (15) and p-VEGFR2, MAPK, and p-MAPK by Western blotting. The protein expression of these receptors were not highly upregulated in any of the HCC cell lines, except for PDGFRβ in HLE and HLF cells (Fig. 2A). A comparable expression level of MAPK was observed among the cell lines, and an increase in p-MAPK expression was observed in HLE cells. The mRNA expression levels of the target receptors *VEGFR1*, *VEGFR2*, *VEGFR3*, *PDGFRA*, *PDGFRB*, *FGFR1*, *FGFR2*, *FGFR3*, and *FGFR4* were determined using real-time RT-PCR in the HUVEC line and the HCC cell line. Higher receptor expression levels were observed for *VEGFR2* in HUVECs, *PDGFRB* in HLE and HLF, *FGFR1* in HUVECs and HLE, *FGFR3* in HepG2, and

FGFR4 in Huh7 (Fig. 2B). The expression levels were consistent with the Western blotting results.

We next evaluated the direct growth inhibitory activity of BIBF 1120 in 4 HCC cell lines *in vitro*. The IC_{50} value of BIBF 1120 for the HLE, HLF, HepG2, and Huh7 cell lines were 2.7 ± 1.7 , 2.7 ± 0.5 , 5.3 ± 0.6 , and 4.3 ± 0.9 μmol/L, respectively (Fig. 2C). These results indicate that the direct growth inhibitory activity of BIBF 1120 against HCC cells was relatively mild (IC_{50} : 2–5 μmol/L).

BIBF 1120 potently inhibits tumor growth and angiogenesis of HCC xenografts *in vivo*

Next, we examined the antitumor and antiangiogenic effects of BIBF 1120 *in vivo*. Mice inoculated with HepG2

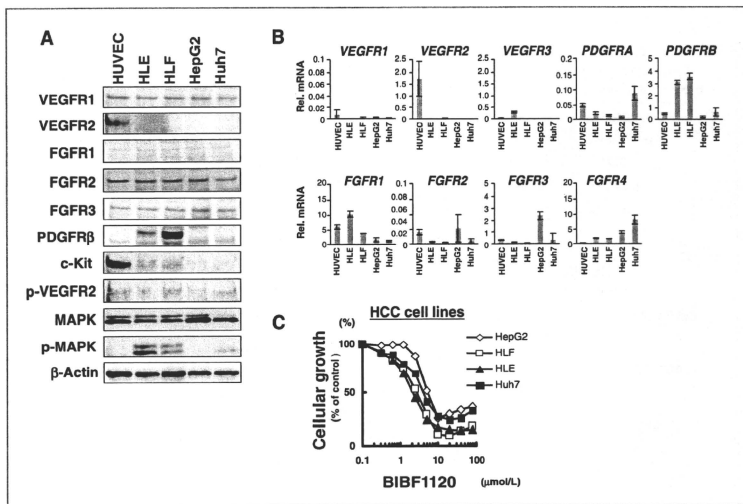


Figure 2. Expression levels of target receptors and sensitivity to BIBF 1120 in HCC cell lines. A, Western blot analysis of the expression levels of VEGFR1, VEGFR2, FGFR1, FGFR2, FGFR3, PDGFR β , c-Kit, p-VEGFR2, MAPK, p-MAPK, and β -actin in HCC cell lines and HUVECs as a control. B, the mRNA expression levels of VEGFR1, VEGFR2, VEGFR3, PDGFR α , PDGFR β , FGFR1, FGFR2, FGFR3, and FGFR4 were determined using real-time RT-PCR. Rel. mRNA, mRNA expression levels normalized using GAPD (target gene/GAPD $\times 10^3$). C, *in vitro* growth inhibitory effect of BIBF 1120 in 4 HCC cell lines by an MTT assay; bars, SD of 3 independent experiments. This assay was conducted in 3 independent experiments.

cells were orally given a low (50 mg/kg/d) or high (100 mg/kg/d) dose of BIBF 1120, or vehicle alone, for 2 weeks (Fig. 3A). The mean tumor volumes on day 14, for each group of mice, were as follows: vehicle alone, $1,367 \pm 634 \text{ mm}^3$; 50 mg/kg/d, $488 \pm 489 \text{ mm}^3$; and 100 mg/kg/d, $572 \pm 556 \text{ mm}^3$. Both doses of BIBF 1120 significantly inhibited tumor growth ($T/C = 0.36$ and 0.42 , respectively), indicating that BIBF 1120 has a potent antitumor activity against HCC *in vivo* (Fig. 3B). Body weight loss was not observed after the administration of BIBF 1120 at either dose (Supplementary Fig. S1). The CD31 staining of tumor tissues showed that BIBF 1120 administration also significantly inhibited tumor angiogenesis (Fig. 3C). Combined with the observation of the direct growth inhibitory activity against HCC *in vitro*, these findings suggest that the antitumor activity of BIBF 1120 *in vivo* mainly result from the drug's antiangiogenic activity, which blocks VEGF signaling.

VEGFR2^{pTyr} PBLs are a pharmacodynamic biomarker *in vivo*

VEGFR2^{CD45^{dim}} PBLs are generally regarded as circulating endothelial cells (22); therefore, we hypothesized that VEGFR2^{CD45^{dim}} PBLs might be useful as a biological

biomarker of VEGFR2 TKIs. The effects of BIBF 1120 on the pTyr levels of VEGFR2^{CD45^{dim}} PBLs and the percentage of VEGFR2^{pTyr} PBLs was examined *in vivo* (Fig. 4A). Murine blood samples were obtained from tumor-bearing, BIBF 1120-treated mice, as described previously. The pTyr levels of the VEGFR2^{CD45^{dim}} PBLs were significantly inhibited by BIBF 1120 treatment, but the difference was relatively small (Fig. 4B and C). On the other hand, the percentage of VEGFR2^{pTyr} PBLs was markedly decreased by BIBF 1120 administration (Cont: $1.8\% \pm 1.1\%$, B50: $0.34\% \pm 0.21\%$, B100: $0.37\% \pm 0.29\%$; Fig. 5A and B). These findings raise the possibility that evaluating the VEGFR2^{CD45^{dim}} PBLs by flow cytometry as a surrogate tissue may contribute to the proof of concept of VEGFR2-targeting drugs or the monitoring of drug effects *in vivo*. Thus, VEGFR2^{pTyr} PBLs might be a useful pharmacodynamic biomarker of VEGFR2 TKIs in early clinical trials.

Discussion

HCC is one of the most hypervascular tumors, and vascular embolization has been used as a therapeutic strategy. A recent study showed that sorafenib exhibits

Kudo et al.

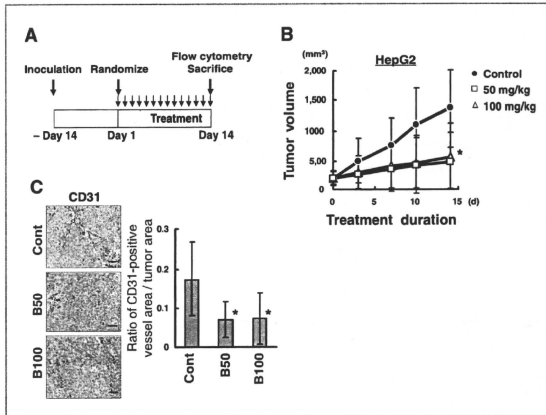


Figure 3. BIBF 1120 exhibited the antitumor and antiangiogenic effects against HCC *in vivo*. **A**, schema of the BIBF 1120 treatment schedules. Mice were inoculated with HepG2 cells for 14 days. The mice were then randomized into 3 groups ($n = 6$ in each group) and treated with BIBF 1120 (50 mg/kg/d, p.o.), BIBF 1120 (100 mg/kg/d, p.o.), or the vehicle control (p.o.) for 14 days. On day 14, the mice were euthanized; blood was collected for the following biomarker study, and tumor specimens were collected for immunohistochemistry. **B**, inhibition of tumor growth by BIBF 1120 treatment. The tumor volume was assessed every 2 to 3 days ($n = 6$ in each group). Bars, SD. *, $P < 0.05$. **C**, inhibition of tumor angiogenesis by BIBF 1120 treatment was evaluated using the CD31 staining of tumor samples. Representative data are shown. MVD was quantified by measuring the number of CD31-positive endothelial cells in the tumors. Ten random fields per tumor sample at a magnification of $\times 200$ were captured and saved for computer-assisted image analysis using the ImageJ software package. The y-axis represents the ratio of the CD31-positive vessel area/tumor area. Scale bar, 100 μ m. Cont, tumor sample treated with vehicle control. B50 and B100, tumor sample treated with BIBF 1120 (50 mg/kg/d, 100 mg/kg/d, p.o.). *, $P < 0.05$.

clinical benefits in patients with advanced HCC (2, 3). This encouraging result suggests that molecular targeting drugs might be active against HCC, especially those that block VEGFR signaling. Our data showed that BIBF 1120 inhibited tumor growth and angiogenesis in HCCs *in vivo*, suggesting that BIBF 1120 may be an active and promising drug against HCC.

BIBF 1120 has a potent inhibitory effect on VEGFRs, similar to that of sorafenib and sunitinib, and it also has activities against FGFRs and Src (refs. 15, 23, 24; Supplementary Table S2). Recent evidence has shown that Src expression is elevated and active in HCC and that Src may play a key role in supporting HCC progression (25); furthermore, Hb α increased the activation of the androgen receptor through c-Src kinase, which acts as a major switch in the activation of HCC (26). We conducted a Western blot analysis to detect the inhibitory effect of BIBF 1120 on Src activity, using HUVECs and HepG2, Huh7, HLE, and HLF cells (Supplementary Fig. S2). The inhibitory effect of BIBF 1120 on p-Src was observed in HUVECs and HLE and HepG2 cells, suggesting that BIBF 1120 actually has an inhibitory effect on Src. This effect may benefit HCC therapy in a manner independent of its antiangiogenic

effect, although this topic needs to be further investigated. Similarly, we showed an inhibitory effect of BIBF 1120 on p-FGFR2 by using FGFR2-amplified gastric cancer cell lines (Supplementary Fig. S3). Brivanib (BMS-540215), a dual inhibitor of VEGFR and FGFR, is currently in development for the treatment of HCC and colon carcinoma, and preclinical studies have shown that FGFR signaling in HCC cells seems to be a promising therapeutic target (27, 28). These results suggest that the effect of BIBF 1120 on FGFR may contribute the antitumor effect, although further investigation is needed.

Numerous candidate biomarkers of angiogenesis have been identified, but the use of these markers for diagnosis, prognosis, and treatment monitoring remains investigational and of uncertain utility (4). Among them, biomarkers for detecting the blockade of VEGFR signaling have received particular attention because of the intimate involvement of this mechanism in drug activity of VEGFR TKIs. We have shown that VEGF-induced VEGFR2^{pTyr} PBLs in peripheral blood samples were markedly decreased by BIBF 1120 treatment *in vivo*. This analysis was done using only peripheral blood collection, VEGF stimulation, and analysis of 2-color flow cytometry; thus, this method is feasible

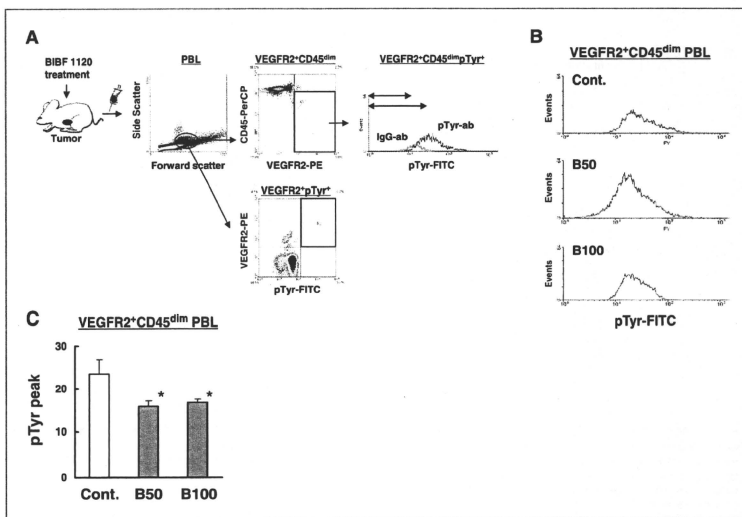


Figure 4. Evaluation of VEGFR2⁺CD45^{dim} PBLs as a biomarker *in vivo*. A, schema of treatment schedules of BIBF 1120 and detection methods. Peripheral blood samples obtained from BIBF 1120-treated mice were stimulated with 20 ng/mL of VEGF for 30 minutes. The cells were fixed, permeabilized, and reacted with the following antibodies: anti-mouse CD45-PerCP, anti-mouse Fli-1-PE, and anti-pTyr-FITC (fluorescein isothiocyanate). Two methods, the tyrosine phosphorylation levels of VEGFR2⁺CD45^{dim} PBLs and the percentage of VEGFR2⁺pTyr⁺ PBLs, were examined. B and C, BIBF 1120 significantly inhibited the pTyr levels of VEGFR2⁺CD45^{dim} PBLs *in vivo*. Cont, blood sample from vehicle control. B50 and B100, blood samples from BIBF 1120 (50 mg/kg/d, 100 mg/kg/d; p.o.) treatment groups; bars, SD. *, *P* < 0.05.

and specific to VEGF signaling. Our method may contribute to the proof of concept for VEGFR2 TKIs and may help to determine the biological optimal dose, especially in phase I clinical trials.

Phase II studies of BIBF 1120 against lung cancer and ovarian cancer have been completed and phase I/II study of BIBF 1120 is currently evaluated in HCC (NCT 01004003). Two large phase III clinical trials against lung cancer

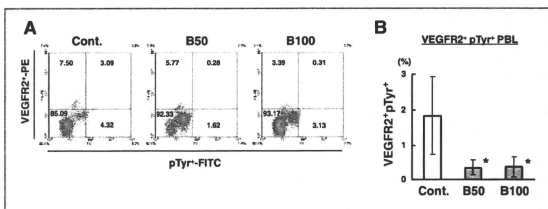


Figure 5. VEGFR2⁺pTyr⁺ PBLs can be used as a pharmacodynamic biomarker *in vivo*. A, the percentage of VEGFR2⁺pTyr⁺ PBLs obtained from BIBF 1120-treated mice. The numeral data indicate the percentage (%) in each quadrant. Representative data are shown. B, BIBF 1120 significantly inhibited the percentage of VEGFR2⁺pTyr⁺ PBLs. Cont, blood samples from vehicle control group (*n* = 6, not treated with drug). B50 and B100, blood samples from BIBF 1120 treatment groups (*n* = 6, 50 mg/kg/d; *n* = 6, 100 mg/kg/d; p.o.); bars, SD. *, *P* < 0.05.

Kudo et al.

(LUME-Lung 1: docetaxel ± BIBF 1120; LUME-Lung 2: pemetrexed ± BIBF 1120) and 1 against ovarian cancer (LUME-Ovar 1: carboplatin/paclitaxel ± BIBF 1120) are now underway. We have shown that BIBF 1120 exhibited antiangiogenic and antitumor activity against HCC *in vivo*. These results may provide the scientific rationale for introducing BIBF 1120 as a treatment of HCC in the future. In addition, our approach of evaluating VEGFR2¹pTyr¹ PBLs in VEGFR TKI might be applicable to future phase I trials. We plan to use this method in clinical settings.

In conclusion, BIBF 1120 clearly inhibited VEGFR2 signaling in endothelial cells and exhibited relatively mild growth inhibitory effects on 4 HCC cell lines (IC₅₀ values: 2–5 μmol/L) *in vitro*. BIBF 1120 exhibited potent anti-tumor and antiangiogenic activities against HCC *in vivo*, and the antitumor effect did not fail or show signs of weakening during the long-term administration period. In addition, VEGFR2¹pTyr¹ PBLs were found to be a noninvasive pharmacodynamic biomarker in a murine model.

References

- Ma WW, Adjei AA. Novel agents on the horizon for cancer therapy. *CA Cancer J Clin* 2009;59:111–37.
- Llovet JM, Ricci S, Mazzaferro V, Hilgard P, Gane E, Blanc JF, et al. Sorafenib in advanced hepatocellular carcinoma. *N Engl J Med* 2008;359:378–90.
- Cheng AL, Kang YK, Chen Z, Tsao CJ, Qin S, Kim JS, et al. Efficacy and safety of sorafenib in patients in the Asia-Pacific region with advanced hepatocellular carcinoma: a phase III randomised, double-blind, placebo-controlled trial. *Lancet Oncol* 2009;10:25–34.
- Brown AP, Citrin DE, Camphausen KA. Clinical biomarkers of angiogenesis inhibition. *Cancer Metastasis Rev* 2008;27:415–34.
- Kummar S, Kinders R, Rubinstein L, Parchment RE, Murgo AJ, Collins J, et al. Compressing drug development timelines in oncology using phase 0 trials. *Nat Rev Cancer* 2007;7:131–9.
- Sessa C, Guibal A, Del Conte G, Ruegg C. Biomarkers of angiogenesis for the development of antiangiogenic therapies in oncology: tools or decoyons? *Nat Clin Pract Oncol* 2008;5:378–91.
- Jubb AM, Hurwitz H, Bai W, Hoimngren EB, Tobin P, Guerrero AS, et al. Impact of vascular endothelial growth factor-A expression, thrombospondin-2 expression, and microvessel density on the treatment effect of bevacizumab in metastatic colorectal cancer. *J Clin Oncol* 2006;24:217–27.
- Poon RT, Fan ST, Wong J. Clinical implications of circulating angiogenic factors in cancer patients. *J Clin Oncol* 2001;19:1207–25.
- George DJ, Halabi S, Shepard FT, Vogelzang NJ, Hayes DF, Small EJ, et al. Prognostic significance of plasma vascular endothelial growth factor levels in patients with hormone-refractory prostate cancer treated on cancer and leukemia group B 9480. *Clin Cancer Res* 2001;7:1932–6.
- Nishimura R, Nagao K, Miyayama H, Matsuda M, Baba K, Yamashita H, et al. Higher plasma vascular endothelial growth factor levels correlate with menopause, overexpression of p53, and recurrence of breast cancer. *Breast Cancer* 2003;10:120–8.
- Werthar K, Christensen IJ, Nielsen HJ. Danish prognostic impact of matched preoperative plasma and serum VEGF in patients with primary colorectal carcinoma. *Br J Cancer* 2002;86:417–23.
- Dreys J, Siegert P, Medinger M, Mross K, Strecker R, Zirgibel U, et al. Phase I clinical study of AZD2171, an oral vascular endothelial growth factor signaling inhibitor, in patients with advanced solid tumors. *J Clin Oncol* 2007;25:3045–54.
- Rini BI, Michalson MD, Rosenberg JE, Bukowski RM, Sosman JA, Stadler WM, et al. Antitumor activity and biomarker analysis of sunitinib in patients with bevacizumab-refractory metastatic renal cell carcinoma. *J Clin Oncol* 2008;26:3743–8.
- Okamoto I, Kaneda H, Satoh T, Okamoto W, Miyazaki M, Morinaga R, et al. Phase I safety, pharmacokinetic, and biomarker study of BIBF 1120, an oral triple tyrosine kinase inhibitor in patients with advanced solid tumors. *Mol Cancer Ther* 2010;9:2825–33.
- Hilberg F, Roth GJ, Krsak M, Kauschitsch S, Sommergruber W, Tontsch-Grunz U, et al. BIBF 1120: triple angiokinase inhibitor with sustained receptor blockade and good antitumor efficacy. *Cancer Res* 2008;68:4774–82.
- Kulimova E, Oelmann E, Bisping G, Kienast J, Meesters RM, Schwäbe J, et al. Growth inhibition and induction of apoptosis in acute myeloid leukemia cells by new indolinone derivatives targeting fibroblast growth factor, platelet-derived growth factor, and vascular endothelial growth factor receptors. *Mol Cancer Ther* 2006;5:3105–12.
- Takeda M, Arazo T, Yokota H, Komatsu T, Yanagihara K, Sasaki H, et al. AZD2171 shows potent antitumor activity against gastric cancer over-expressing fibroblast growth factor receptor 2/keratinocyte growth factor receptor. *Clin Cancer Res* 2007;13:3051–7.
- Arazo T, Fukumoto H, Takeda M, Tamura T, Saijo N, Nishio K. Small in-frame deletion in the epidermal growth factor receptor as a target for ZD6474. *Cancer Res* 2004;64:9101–4.
- Arazo T, Yanagihara K, Takigahira M, Takeda M, Koizumi F, Shiratori Y, et al. ZD6474 inhibits tumor growth and intraperitoneal dissemination in a highly metastatic orthotopic gastric cancer model. *Int J Cancer* 2006;118:483–9.
- Márquez MG, Galeano A, Olmos S, Roux ME. Flow cytometric analysis of intestinal intraepithelial lymphocytes in a model of immunodeficiency in Wistar rats. *Cytometry* 2000;41:115–22.
- Zanzer F, Blana A, Gaumann A, Stolzenberg JU, Rabenalt R, Bach T, et al. Topographical anatomy of prostatic and capsular nerves: quantification and computerized planimetry. *Eur Urol* 2009;54:353–60.
- Bertolini F, Shaked Y, Mancuso P, Kerbel RS. The multifaceted circulating endothelial cell in cancer: towards marker and target identification. *Nat Rev Cancer* 2006;6:835–45.
- Wilhelm SM, Carter C, Tang L, Wilkie D, McNabola A, Rong H, et al. BAY 43-9006 exhibits broad spectrum oral antitumor activity and targets the RAF/MEK/ERK pathway and receptor tyrosine kinases involved in tumor progression and angiogenesis. *Cancer Res* 2004;64:7099–109.
- Mendel DB, Laird AD, Xin X, Louie SG, Christensen JG, Li G, et al. *In vivo* antitumor activity of SU11248, a novel tyrosine kinase inhibitor

Disclosure of Potential Conflicts of Interest

No potential conflicts of interest were disclosed.

Acknowledgment

We thank Mr. Shinji Kurashimo (Life Science Research Institute, Kinki University) for technical assistance.

Grant Support

This work was supported by funds for the Comprehensive Third Term of the 10-Year Strategy for Cancer Control, the program for the promotion of Fundamental Studies in Health Sciences of the National Institute of Biomedical Innovation (NIBio), a grant-in-aid for Scientific Research from the Ministry of Education, Culture, Sports, Science and Technology of Japan (19299018), and a fund from the Health and Labor Scientific Research Grants (09-9).

The costs of publication of this article were defrayed in part by the payment of page charges. This article must therefore be hereby marked advertisement in accordance with 18 U.S.C. Section 1734 solely to indicate this fact.

Received October 15, 2009; revised October 1, 2010; accepted November 24, 2010; published OnlineFirst December 23, 2010.

- targeting vascular endothelial growth factor and platelet-derived growth factor receptors: determination of a pharmacokinetic/pharmacodynamic relationship. *Clin Cancer Res* 2003;9:327-37.
25. Lau GM, Lau GM, Yu GL, Gelman IH, Gutowski A, Hangauer D, et al. Expression of Src and FAK in hepatocellular carcinoma and the effect of Src inhibitors on hepatocellular carcinoma *in vitro*. *Dig Dis Sci* 2009;54:1465-74.
26. Yang WJ, Chang CJ, Yeh SH, Lin WH, Wang SH, Tsai TF, et al. Hepatitis B virus X protein enhances the transcriptional activity of the androgen receptor through c-Src and glycogen synthase kinase-3beta kinase pathways. *Hepatology* 2009;49:1515-24.
27. Marathe PH, Kamath AV, Zhang Y, D'Arienzo C, Bhide R, Fargnoli J. Preclinical pharmacokinetics and *in vitro* metabolism of brivanib (BMS-540215), a potent VEGFR2 inhibitor and its alanine ester pro-drug brivanib alaninate. *Cancer Chemother Pharmacol* 2009;65:55-66.
28. Huynh H, Ngo VC, Fargnoli J, Ayers M, Soo KC, Koong HN, et al. Brivanib alaninate, a dual inhibitor of vascular endothelial growth factor receptor and fibroblast growth factor receptor tyrosine kinases, induces growth inhibition in mouse models of human hepatocellular carcinoma. *Clin Cancer Res* 2008;14:6146-53.

Three-gene predictor of clinical outcome for gastric cancer patients treated with chemotherapy

HK Kim^{1,2}, IJ Choi², CG Kim²,
HS Kim², A Oshima¹, Y Yamada³,
T Arao⁴, K Nishio⁴,
A Michalowski¹ and JE Green¹

¹Laboratory of Cancer Biology and Genetics, National Cancer Institute, Bethesda, MD, USA; ²National Cancer Center, Goyang, Gyeonggi, Republic of Korea, ³National Cancer Center, Tokyo, Japan and ⁴Kinki University School of Medicine, Osaka-Sayama, Japan

Correspondence:

Dr JE Green, Laboratory of Cancer Biology and Genetics, National Cancer Institute, 37 Convent Drive, Bethesda, MD 20892, USA.
E-mail: JEGreen@mail.nih.gov

To identify transcriptional profiles predictive of the clinical benefit of cisplatin and fluorouracil (CF) chemotherapy to gastric cancer patients, endoscopic biopsy samples from 96 CF-treated metastatic gastric cancer patients were prospectively collected before therapy and analyzed using high-throughput transcriptional profiling and array comparative genomic hybridization. Transcriptional profiling identified 917 genes that are correlated with poor patient survival after CF at $P < 0.05$ (poor prognosis signature), in which protein synthesis and DNA replication/recombination/repair functional categories are enriched. A survival risk predictor was then constructed using genes, which are included in the *poor prognosis signature* and are contained within identified genomic amplicons. The combined expression of three genes—*MYC*, *EGFR* and *FGFR2*—was an independent predictor for overall survival of 27 CF-treated patients in the validation set (adjusted $P = 0.017$), and also for survival of 40 chemotherapy-treated gastric cancer patients in a published data set (adjusted $P = 0.026$). Thus, combined expression of *MYC*, *EGFR* and *FGFR2* is predictive of poor survival in CF-treated metastatic gastric cancer patients.

The Pharmacogenomics Journal (2010) 0, 000–000. doi:10.1038/tpj.2010.87

Keywords: gastric; cancer; chemotherapy; gene; expression

Introduction

Although the emerging area of targeted anticancer agents holds great promise, cytotoxic chemotherapy remains the primary treatment option for many cancer patients. Identifying patients who likely will or will not benefit from cytotoxic chemotherapy through the use of biomarkers could greatly improve clinical management by better defining appropriate treatment options for patients. None of the molecules experimentally identified to cause chemotherapy resistance *in vitro* was sufficiently validated in primary tumors and thus clinically applicable,¹ underscoring the importance of well-designed, clinical study to identify clinically relevant mechanisms for chemotherapy resistance. In fact, however, such predictors derived to date from high-throughput transcriptional profiling of primary tumors, especially gastrointestinal tract cancers, have not shown satisfactory performance.^{2–5} It may be primarily owing to the high rate of false-positive discovery in high-throughput data, in addition to the high degree of genetic variation of individual tumor compared with limited number of samples available for the study.

To provide insight into clinically relevant mechanisms for chemotherapy resistance in gastric cancer, we prospectively collected and analyzed 123 endoscopic biopsy samples before cisplatin and fluorouracil (CF) chemotherapy from patients with extended follow-up, using high-throughput transcriptional profiling and comparative genomic hybridization (CGH) analyses. We could identify functional categories enriched in genes correlated with patient outcome, and develop a genomic predictor that was validated in two independent data sets.

Materials and methods

Patients

Sample collection, treatment and follow-up were performed according to a protocol approved by the Institutional Review Board of the National Cancer Center Hospital in Goyang, Korea (NCCNH501-003). All patients signed an Institutional Review Board-approved informed consent form. Eligibility for enrollment into the study included the following parameters: (1) age ≥ 18 years; (2) histologically confirmed gastric adenocarcinoma; (3) clinically documented distant metastasis; (4) no previous or concomitant malignancies other than the gastric cancer; (5) no previous history of chemotherapy, either adjuvant or palliative; and (6) adequate function of all major organs. Patients who were lost to follow-up before completing six cycles of chemotherapy, except for documented progressive disease, were excluded from this study.

Sample size calculation

Overall survival was the primary clinical end point of this study. As a minimum of 91 events were estimated to be required for the number of training set samples⁹ at $\alpha = 0.001$, $\beta = 0.05$, τ (standard deviation of log intensity) = 0.75 and δ (hazard ratio (HR) associated with one-unit change of log intensity) = 2, we used the 96 samples collected until January 2005 as the training set for development of the predictor.

Ninety-six eligible patients who were treated with CF by one medical oncologist (HK) from August 2001 to January 2005 were used for the expression profiling training set. A second group of 27 eligible patients was used as the array validation cohort. Twenty-two patients in the validation cohort were treated with CF, and five patients were treated with cisplatin plus oral capecitabine (a fluorouracil pro-drug considered equivalent to fluorouracil; CX),⁷ by another group of medical oncologists in the same institution between February 2005 and April 2006. Tissue procurement and processing were the same for the training and validation samples.

Treatment

Patients continued therapy indefinitely until they experienced unacceptable toxicities or progressive disease was documented. CF-treated patients received cisplatin 60 mg m⁻² intravenously on day 1 and fluorouracil 1000 mg m⁻² intravenously on days 1–5 of a 3-week

schedule. The treatment schedule for fluorouracil could be shortened at the discretion of the oncologist to 3 instead of 5 days for elderly patients (≥ 70 years) or patients with poor performance status (Eastern Cooperative Oncology Group performance status ≥ 2). Chemotherapy doses were reduced according to toxicities and the patient's performance status. Specific dose modification schemes for the subsequent cycle were left to the discretion of treating oncologist. Five patients (18.5%) in the validation group received oral capecitabine (Xeloda; Roche; 1250 mg m⁻² twice a day for 2 weeks) instead of intravenous infusion of fluorouracil. Time to progression was measured from the initiation of chemotherapy to the progressive disease. In patients without any measurable lesions, time to progression was measured to the time when a change in therapy was required because unmeasurable lesions (such as ascites) unequivocally progressed.

Gene expression and CGH microarray analyses

Tissue samples were collected and processed for RNA and DNA extraction as described previously,⁸ only if samples contained at least 50% tumor cells. Affymetrix (Santa Clara, CA, USA) HG-U133A gene expression microarray data were analyzed with survival analysis algorithms of BRB-Array-Tools (version 3.6, National Cancer Institute, <http://linus.nci.nih.gov/BRB-ArrayTools.html>).⁹ The survival risk groups were constructed using a predictive index based on the supervised principal component method of Bair and Tibshirani.¹⁰ A three-gene predictive index percentile was generated based on the weighted average of the log intensities of the three genes (*FGFR2* (211401_s_at), *EGFR* (210984_x_at) and *c-MYC* (202431_s_at)), using a proportional hazards regression on the first two principal components of the log intensities of those three genes, in which a high value of the predictive index corresponds to a high risk of death. If the predictive index of a sample in the validation set corresponded to the median predictive index of the training set, the sample was assigned a 50% predictive index. We specified the number of risk groups as 2 (high and low) and the predictive index percentile for defining the two risk groups as 67%, using a 67.1% rate of clinical benefit (partial response and stable disease) and 32.9% rate of progressive disease in the training set. We also performed Cox regression analyses using this three-gene predictive index percentile as a continuous variable, in which HRs for survival were calculated according to each percentile increase in three-gene predictive index percentile (from 0 to 100%). Array CGH data were generated using Agilent (Santa Clara, CA, USA) 4 × 44k HD-CGH Microarrays and analyzed using CGH Analytics software (version 3.5.14). Aberrations with average tumor/normal log₂ ratio > 2.0 were defined as amplifications. Experimental details are provided in Supplementary Materials and Methods.

Analyses of published DNA microarray data

The entire set of published Affymetrix U133 Plus 2.0 DNA microarray data⁴ ($n = 40$) was combined with our training set data ($n = 96$), using common probe set IDs. MASS data of

the combined data set were \log_2 transformed, normalized using the median over the entire arrays and analyzed for survival risk prediction using BRB-ArrayTools 3.6, as described above.

Publicly accessible microarray data for surgically treated gastric cancer patients generated by the Stanford Functional Genomics Facility were obtained from the NCBI GEO database (GSE4007) and included about 30 300 genes common to these data sets. The microarray data were generated and normalized as described in Leung *et al.*¹¹ Batch effects in gene expression were removed with probe-wise mean centering and missing data were imputed with the nearest-neighbor averaging method.¹² The array cDNA clones were annotated using SOURCE (Stanford Microarray Database) and the Entrez GeneID was used as the mapping identifier for the Affymetrix HG-U133A array. A combined data set of our training set data ($n=96$) and GSE4007 data ($n=88$) was analyzed for survival risk prediction using BRB-ArrayTools 3.6 as described above.

Results

Genes correlated with poor survival after CF therapy

As primary gastric cancer lesions cannot be reliably measured by diagnostic imaging, patient survival, not radiographic response, was used as the primary clinical covariate to which gene expression was correlated to identify a predictor of response to CF therapy. To define a gene expression signature that correlates with overall survival, we used expression array data of 96 pretreatment biopsy samples as the training set to develop a predictor. Ninety-five out of 96 patients (99%) in the training set cohort died with follow-up for one survivor at 38.9 months. None of the clinicopathological or treatment factors listed in Table 1, including second-line chemotherapy, were significantly correlated with survival time of the patients in the training set.

To identify a transcriptional profile related to clinical benefit from CF therapy, the survival times of patients in the array training set were correlated with the mRNA expression levels measured by microarray. One thousand five hundred and sixty-five genes were significantly correlated with the overall survival of the 96 patients (P -value < 0.05). Among them, 917 genes had an HR higher than 1 (poor prognosis signature) and 648 genes had an HR lower than 1 (good prognosis signature). We performed gene ontology analysis on this 'poor prognosis signature' using Ingenuity Pathway Analysis (www.ingenuity.com). The role of *BRCA1* in DNA damage response (*BRCA2*, *E2F5*, *FANCE*, *MSH2*, *NBN*, *PLK1*, *RFC*, *SMARCA4*, *SLC19A1*), nucleotide excision repair (*ERCC2*, *POLR2C*, *POLR2J*, *POLR2J2*, *RAD23A*, *RAD23B*) and estrogen receptor signaling were highly represented canonical pathways. Many of these *poor prognosis signature* genes belonging to these three pathways are previously linked to *in vitro* cisplatin resistance.¹³⁻¹⁵ Overexpression of *ERCC2* ($P=0.007$ in our data) is associated with cisplatin resistance in lung cancer cell lines.¹³ Silencing of *hHR23A* ($P=0.022$ in our

Table 1 Clinicopathological characteristics of patients

	Training set ($n=96$)	Validation set ($n=27$)
Baseline clinicopathological characteristic		
Age, no. (%)		
< 70 years	90 (93.8%)	25 (92.6%)
≥ 70 years	6 (6.2%)	2 (7.4%)
Sex, no. (%)		
Male	73 (76.0%)	23 (85.2%)
Female	23 (24.0%)	4 (14.8%)
PS, no. (%)		
ECOG PS 0 or 1	91 (94.8%)	25 (92.6%)
ECOG PS 2 or 3	5 (5.2%)	2 (7.4%)
Histological type, no. (%)		
Lauren's intestinal	40 (41.7%)	9 (33.3%)
Lauren's diffuse	56 (58.3%)	18 (66.6%)
Location of primary lesion, no. (%)		
Upper 1/3	14 (14.6%)	2 (7.4%)
Middle 1/3	28 (29.2%)	10 (37.0%)
Lower 1/3	49 (51.0%)	15 (55.6%)
Entire stomach	5 (5.2%)	0
Distant metastasis, no. (%)	96 (100%)	27 (100%)
Tumor cell percentage in sample (%)		
Median	60	70
Interquartile range	50-70	55-80
Treatment and outcome		
Chemotherapy regimen, no. (%)		
Cisplatin/fluorouracil	96 (100%)	22 (81.5%)
Cisplatin/capecitabine	0 (0%)	5 (18.5%)
Relative dose intensity (%)		
Median	79	81
Interquartile range	73-88	72-87
Number of chemotherapy cycles		
Median	4	7
Interquartile range	3-9	5-13
Response (WHO criteria), no. (%)		
PR	38 (44.7%)	12 (48.0%)
SD	19 (22.4%)	9 (36.0%)
PD	28 (32.9%)	4 (16.0%)
Non-measurable disease	11	2
Second-line chemotherapy, no. (%)	69 (71.9%)	19 (70.4%)
Median follow-up for survivors (months)	39.4	30.4
Overall survival (months)		
Median	8.1	12.6
Interquartile range	5.6-15.9	7.4-30.4
Time to progression (months)		
Median	3.9	6.3
Interquartile range	2.2-8.3	3.9-14.6

Abbreviations: ECOG, Eastern Cooperative Oncology Group; PD, progressive disease; PR, partial response; PS, performance status; SD, stable disease; WHO, World Health Organization.

data) decreases the nuclear DRP1 level and cisplatin resistance in lung adenocarcinoma cells.¹⁴ Fanconi anemia-BRCA pathway is reported in cisplatin-sensitive ovarian tumors.¹⁵ Thus, this gene ontology analysis supports the clinical relevance of these DNA repair canonical

pathways, which were shown to be associated with *in vitro* cisplatin resistance.

Q2 Infinitesimal perturbation analysis functional categories enriched in poor prognosis signature were: protein synthesis, DNA replication/recombination/repair and cancer (Supplementary Table 2). The protein synthesis category includes ribosomal subunit mRNAs (*RPL13*, *RPL18*, *RPL24*, *RPL30*, *RPL38*, *RPL5*, *RPL7*, *RPL7A*, *RPL8*, *RPS2*, *RPS5*) and eukaryotic translation initiation factors (*EIF1*, *EIF2B2*, *EIF2B4*, *EIF2S1*, *EIF3B*, *EIF3C*, *EIF3D*, *EIF3E*, *EIF3F*, *EIF3H*, *EIF3I*, *EIF4A1*, *EIF4A3*, *EIF4B*, *EIF4EBP1*, *EIF5*, *EIF5B*). This result suggests that the most prominent feature of poor prognosis signature is increased protein synthesis, presumably resulting from activation of oncogenes, such as *EGFR*, *FGFR2* and *MYC* (Supplementary Table 2). *MYC*-induced transcriptional activation of protein synthesis-related genes is previously shown by a microarray report that the majority of genes responsive to *MYC* overexpression are involved in macromolecular synthesis, protein turnover and metabolism, including 30 ribosomal protein genes.¹⁶

Infinitesimal perturbation analysis canonical pathways enriched in 648 genes in good prognosis signature were antigen presentation pathway, B-cell development and interleukin-15 production. Enriched functional categories were gastrointestinal disease, inflammatory disease and genetic disorder.

Development of the three-gene predictor

Although such a gene ontology analysis of the whole signature provides some insight into clinically relevant mechanisms for chemotherapy resistance, this large number of genes is not readily amenable to clinical application. Therefore, we wished to narrow down 917 genes in the whole poor prognosis signature to the smaller number of genes, which may have driven the expression of majority of genes in the signature. Focusing on such 'driver gene' candidates would also minimize the chance of including false-positive discovery in a genomic predictor. For this purpose, a second tier of genomic analysis was performed to identify genes that could be functionally important in gastric cancer cells.

Genomic DNA from samples available from the training set patients was analyzed by array CGH to identify gene amplifications. Age, sex and overall survival were similar between the 30 patients (31.3%) whose samples were analyzed by array CGH and the other patients in the training set. Using very conservative criteria (average tumor/normal log₂ ratio >2.0 for ≥5 consecutive CGH probes), nine amplicons were identified in 11 patients (Table 2). We identified genes found in both the 1565 gene expression signature whose transcriptional levels correlated with poor survival of 96 training set patients (*P*-value <0.05) and that are also located within the nine amplicons identified by the array CGH. Three genes—*MYC* (8q24.13–24.21), *EGFR* (7p11.2) and *FGFR2* (10q26)—were identified in the amplicons (Table 2) whose expression array signal values significantly correlated with the survival time of the 96 patients in the training set (Figure 1). Patients with *EGFR*

Table 2 Amplicons identified using array CGH*

Cytoband	Start	End	Target gene	No. of patients
3q27.1	185 763 900	185 763 959	<i>EPHB3</i>	1
5q33.1	149 481 646	149 514 673	<i>PDGFRB</i>	1
7p11.2	54 746 103	55 363 004	<i>EGFR</i>	1
8q24.13–24.21	126 357 675	128 822 455	<i>MYC</i>	2
9p13.3	33 745 689	33 961 753	<i>PRSS3</i> , <i>UBE2R2</i> , <i>UBAP2</i>	1
10q26	123 264 724	13 123 458 467	<i>FGFR2</i>	2
17q12	35 046 052	35 282 145	<i>ERBB2</i>	2
17q21.2	36 110 139	36 230 022	<i>KRT24</i> , <i>KRT25A</i> , <i>KRT25C</i> , <i>KRT25D</i> , <i>KRT10</i>	2
17q21.2	36 569 493	36 888 515	<i>KRTAP4-4</i> , <i>KRTAP4-10</i> , <i>KRTAP9-9</i> , <i>KRTAP9-4</i> , <i>KRTAP17-1</i> , <i>KRTHA3A</i> , <i>KRTHA3B</i> , <i>KRTHA4</i> , <i>KRTHA1</i> , <i>KRTHA7</i> , <i>KRTHA8</i> , <i>KRTHA2</i> , <i>KRTHAS</i>	1

Abbreviation: CGH, comparative genomic hybridization.

*Defined by aberrations with average tumor/normal log₂ ratio >2.0 for ≥5 consecutive probes.

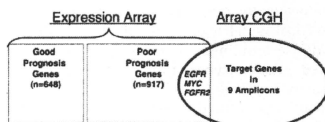


Figure 1 Three genes—*EGFR*, *FGFR2* and *MYC*—overlap between genes whose array expression levels correlated with survival times (96 training set patients, *P*<0.05) and gene copy number changes determined by array comparative genomic hybridization (CGH) (tumor/normal log₂ ratio >2 for ≥5 consecutive probes).

and *FGFR2* amplifications had higher expression levels of each gene (8.4 and 10.2 ± 0.8 (mean ± s.d.), for *EGFR* and *FGFR2*, respectively) than tested patients without the amplification of these genes (5.9 ± 1.0 and 5.2 ± 1.1, for *EGFR* and *FGFR2*, respectively). One of the two patients with *MYC* amplification had higher expression than patients without amplification (10.9 vs 9.5 ± 0.9).

The mRNA expression array signal values of these three genes were correlated with the short survival time with *P*-values of 0.0154, 0.0096 and 0.0057, for *MYC*, *EGFR* and *FGFR2*, respectively. The expression patterns of these three

genes along with the cumulative survival data for all patients are depicted in the heatmap in Figure 2. None of the three genes had significantly different expression levels between those patients who received second-line chemotherapy and those who did not. Quantitative real-time RT-PCR and immunohistochemical staining for the three genes validated the array expression data (Supplementary Figures 1 and 2).

A three-gene predictive index percentile was then calculated for each of the 27 patients in the validation cohort, based on the weighted average of the log intensities of these three genes for each sample (designated as the three-gene

predictor). Patterns of *MYC*, *EGFR* and *FGFR2* expression in these 27 patients, together with the predictive index, are graphically displayed in Figure 2. As a continuous variable, the three-gene predictive index percentile is an independent predictor for poor survival in the validation set by Cox regression analyses, after considering age, performance status, histological type and second-line chemotherapy (adjusted $P=0.017$) (Table 3). Patients predicted to have poor survival after CF using a predictive index percentile $\geq 67\%$ had a significantly shorter median survival than patients with a predictive index percentile $< 67\%$ (7.4 months for the high-risk group vs 16.8 months for the

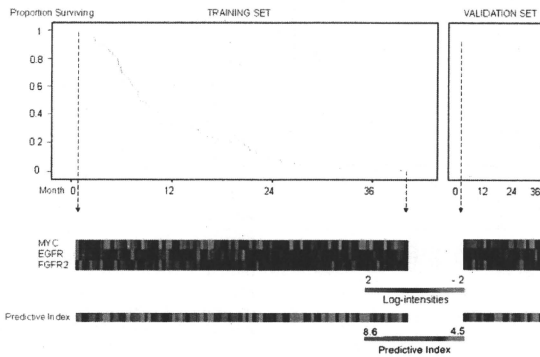


Figure 2 Affymetrix array expression levels of *MYC*, *EGFR* and *FGFR2* in 96 training set samples (left) and 27 validation set samples (right), shown with Kaplan-Meier plots for overall survival. Samples are ordered by the increasing survival period of patient from left to right, for the training and validation sets, respectively. A three-gene predictive index for each patient based on the three-gene predictor is indicated below.

Table 3 Cox regression analyses of the three-gene predictive index percentile, as a continuous variable, for 27 patients in the validation set

	Overall survival		Time to progression	
	P-value	HR (95% CI)	P-value	HR (95% CI)
Univariate				
Three-gene predictive index percentile*	0.050	1.015 ^b (1.000–1.030)	0.026	1.017 (1.002–1.031)
Multivariate				
Three-gene predictive index percentile	0.017	1.023 (1.004–1.042)	0.014	1.023 (1.005–1.043)
Age ≥ 70 years ^c	0.027	7.614 (1.257–46.130)	0.144	3.605 (0.646–20.112)
Poor performance status (ECOG PS 2 or 3)	0.346	2.130 (0.442–10.258)	0.074	4.829 (0.861–27.086)
Second-line chemotherapy	0.041	4.231 (1.064–16.831)	0.011	5.992 (1.502–23.902)
Diffuse histological type	0.773	1.164 (0.415–3.263)	0.280	1.774 (0.626–5.025)

Abbreviations: CI, confidence interval; ECOG PS, Eastern Cooperative Oncology Group performance status; HR, hazard ratio.

*Computed based on weighted average of log intensities of the three genes (*EGFR*, *FGFR2* and *MYC*) obtained using a proportional hazards regression on the first two principal components of the log signal intensities of those three genes.

^bHR for each percentile increase in three-gene predictive index percentile. For example, a predictive index percentile of 100 (the highest predictive index) is associated with an HR of 4.4 ($= 1.015^{100}$), compared with a predictive index percentile of 0 (the lowest predictive index). The median predictive index (50%) is associated with HRs of 2.1 ($= 1.015^{50}$), compared with the lowest predictive index.

^cFor patients aged ≥ 70 years, the treatment schedule for fluorouracil could be shortened at the discretion of the oncologist to 3 instead of 5 days.

low-risk cohort; $P=0.047$) (Figure 3a). As a class, the high-risk group predicted by the three-gene predictor (patient group with a predictive index percentile $\geq 67\%$) was associated with an adjusted HR of 3.1 (95% CI, 1.2–8.4;

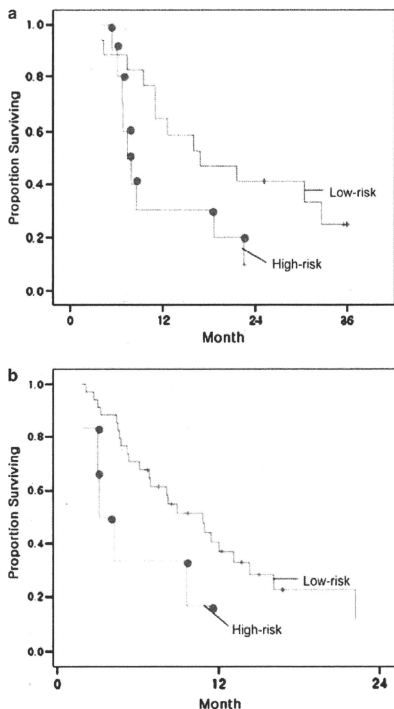


Figure 3 (a) Kaplan–Meier survival curves for the two risk groups of the validation cohort predicted by three-gene predictor. Patients at a high risk (predictive index percentile $\geq 67\%$; $n=10$) had significantly shorter median survival than patients at a low risk ($n=17$) (7.4 vs 16.8 months; log rank $P=0.047$). Green and blue lines represent overall survival curves for the predicted high- and low-risk groups, respectively. (b) Kaplan–Meier survival curves for the two risk groups of the published microarray data set from 40 metastatic gastric cancer patients treated with either fluorouracil-based regimens or cisplatin/irinotecan combination chemotherapy regimen. Patients at a high risk (predictive index percentile $\geq 67\%$; $n=6$) had shorter median survival than patients at a low risk ($n=34$), at a borderline significance (3.1 vs 10.8 months; log rank $P=0.056$). Green and blue lines represent overall survival curves for the predicted high- and low-risk groups, respectively. The color reproduction of the figure is available on the html full text version of the manuscript.

$P=0.022$). In addition, the three-gene predictive index percentile is also an independent predictor for the time to progression, which is a more specific indicator of the clinical responsiveness to systemic therapy than overall survival¹⁷ (adjusted $P=0.014$) (Table 3). We therefore show that, independent of old age (≥ 70 years), poor performance status (Eastern Cooperative Oncology Group performance status ≥ 2) and second-line chemotherapy, the three-gene predictive index is predictive of the benefit from CF to metastatic gastric cancer patients. An adjusted HR for time to progression according to each percentile increase in three-gene predictive index percentile was 1.023 (95% CI, 1.005–1.043) (that is, 100, 75 and 50% predictive indices are associated with an HR of 9.7 ($=1.023^{100}$), 5.5 ($=1.023^{75}$) and 3.1 ($=1.023^{50}$), respectively, compared with a 0% predictive index).

Three-gene predictor predicts survival of patients in the second validation set

To extend these results, we wished to test the predictive power of the three-gene predictor in other independent data sets. After the three-gene predictor was validated in 27 patient samples in our validation set, another microarray study with a comparable study design to our study was published in the literature.⁴ These data were only one published microarray data set that could be used to determine whether the three-gene predictor could predict the outcome of metastatic gastric cancer patients treated with either cisplatin or fluorouracil. This data set contains pretreatment expression array data for 40 patients who subsequently received either fluorouracil-based chemotherapy ($n=24$) or cisplatin/irinotecan combination chemotherapy ($n=16$) and patient survival data. We applied the same three-gene predictor to this published microarray data set, just as we did to our 27 patient data in the first validation set. The three-gene predictive index percentile, as a continuous variable, was found to be significantly associated with poor survival of these 40 patients ($P=0.047$; HR according to each percentile increase in three-gene predictive index percentile = 1.014 (95% confidence interval, 1.000–1.027)). Cox multivariate analysis showed that the three-gene predictive index percentile is an independent predictor for poor survival, after considering performance status, age, sex and the chemotherapy regimen (adjusted $P=0.026$; adjusted HR = 1.017 (1.002–1.032)) (Table 4, Figure 3b). Thus, the predictive power of the three-gene predictor is consistent across two validation sets, that is, one from our study patients and the other from published data.

Interestingly, the three-gene predictor was found to be an independent predictor for poor survival, when the same Cox regression analysis was performed only on a subset of these patients ($n=16$) treated with cisplatin in combination with irinotecan, a topoisomerase I inhibitor (adjusted $P=0.011$; adjusted HR = 1.038 (1.008–1.068)). Patients treated with irinotecan were not included in the original training set patients. Hence, the predictive power of three-gene predictor may not be specifically associated with only CF therapy, although further large-scale studies need to be

performed to address the predictive value of the three-gene predictor for other therapeutic regimens.

Three-gene predictive index and radiographic response

Although the radiographic tumor response was not the main end point of this study, we also evaluated the association between the three-gene predictive index and radiographic response of patients with measurable disease. When published data^a were also included, 104 patients had either

partial response or stable disease (clinical benefit) as the best response, whereas 46 patients had progressive disease. The three-gene predictive index was significantly associated with radiographic response at a univariate *P*-value of 0.039, which is higher than the Cox regression *P*-value for the overall survival of all study patients (Table 5). This statistical association was at borderline significance in a multivariate regression analysis.

Three-gene predictor is not prognostic but predictive

Although we showed that the three-gene predictor predicted time to progression and overall survival for CF-treated patients, we wished to further address whether it represents a prognostic signature, using the published data set from 88 gastric cancer patients who were treated by surgery alone and not with chemotherapy.¹¹ The three-gene predictive index percentile was not a prognostic factor in this data set as a continuous variable (*P* = 0.506). There was no difference in survival in the surgically treated patients between the high- and low-risk groups predicted by the three-gene predictor (*P* = 0.972). These results strongly suggest that the three-gene predictor is not a predictor of prognosis for gastric cancer patients, but is predictive of the patient response to chemotherapy.

Table 4 Cox regression analyses of the three-gene predictive index percentile, as a continuous variable, for published DNA microarray data from 40 metastatic gastric cancer patients treated with either FU-based chemotherapy or cisplatin/irinotecan combination chemotherapy

	Overall survival	
	<i>P</i> -value	HR (95% CI)
<i>Univariate</i>		
Three-gene predictive index percentile	0.047	1.014 (1.000–1.027)
<i>Multivariate</i>		
Three-gene predictive index percentile	0.026	1.017* (1.002–1.032)
Performance status ≥ 1	0.028	3.008 (1.129–8.016)
Age ^b	0.766	0.995 (0.961–1.030)
Male	0.538	1.359 (0.512–3.605)
FU-based chemotherapy regimen ^c	0.744	0.854 (0.332–2.199)

Abbreviations: CI, confidence interval; FU, fluorouracil; HR, hazard ratio.
^aAdjusted HR for each percentile increase in three-gene predictive index percentile. For example, a predictive index percentile of 100 (the highest predictive index) is associated with an HR of 5.4 (*P* = 1.017⁹⁹), compared with a predictive index percentile of 0 (the lowest predictive index).
^bAs a continuous variable.
^cAs compared with the irinotecan/cisplatin combination chemotherapy regimen.

Discussion

Cytotoxic chemotherapy prolongs the median survival of metastatic gastric cancer patients from 3–5 to 9–11 months compared with best supportive care, with a response rate of 40–50%.^{18–21} Combination CF constitutes the backbone for chemotherapy regimens commonly used for gastric cancers.^{19,22} We also reported that CF in combination with low-dose docetaxel is active for metastatic gastric cancer with tolerable toxicity profile.¹⁸ The ability to predict the primary resistance of common solid tumors to cytotoxic

Table 5 Logistic regression analysis on the three-gene predictive index for radiographic response of 150 patients with measurable disease, including patients represented by the published data set

	Radiographic response ^a		Time to progression		Overall survival	
	<i>P</i> -value	OR (95% CI)	<i>P</i> -value ^b	HR (95% CI)	<i>P</i> -value ^c	HR (95% CI)
<i>Univariate</i>						
Three-gene predictive index ^d	0.039	2.001 (1.036–3.864)	0.020	1.304 (1.042–1.631)	0.030	1.288 (1.026–1.618)
<i>Multivariate</i>						
Three-gene predictive index	0.059	1.902 (0.976–3.704)	0.019	1.309 (1.045–1.641)	0.018	1.316 (1.048–1.654)
Age ≥ 70 years	0.914	1.069 (0.318–3.598)	0.791	1.119 (0.486–2.577)	0.113	1.600 (0.895–2.862)
Poor performance status (ECOG PS 2 or 3)	0.336	0.513 (0.132–1.999)	0.026	2.192 (1.097–4.381)	0.048	1.921 (1.004–3.677)

Abbreviations: CI, confidence interval; ECOG PS, Eastern Cooperative Oncology Group performance status; HR, hazard ratio; OR, odds ratio; WHO, World Health Organization
^aNo clinical benefit (progressive disease according to the WHO criteria; *n* = 46) vs clinical benefit (partial response and stable disease; *n* = 104).
^bResult of Cox regression analysis on the three-gene predictive index for the time to progression of 123 patients in the training and the first validation sets.
^cResult of Cox regression analysis on the three-gene predictive index for the overall survival of all 163 study patients including published data set.
^dComputed based on weighted average of log intensities of the three genes (*EGFR*, *FGFR2* and *MYC*) obtained using a proportional hazards survival regression on the first two principal components of the log signal intensities of those three genes.

chemotherapy is currently lacking, but would significantly improve patient care by identifying those who would best be treated by alternative strategies. This study has identified a three-gene predictor that distinguishes gastric cancer patients likely to receive a therapeutic benefit from CF from those who will not.

Most previous studies attempting to identify predictors of chemoresistance in gastric cancer have examined only individual genes such as *TS* or *ERCC1*.^{23,24} High-throughput DNA microarray analyses to identify gene expression signatures predictive of chemotherapy or chemoradiotherapy resistance in gastrointestinal cancer patients have been limited by the small number of samples,^{2,3} heterogeneous treatment⁴ or were not prospectively designed.⁵ In contrast to these previous studies, our study uses high-throughput genomic approaches, is prospective with a large, pre-defined number of training set patients, separate validation cohorts and survival data during an extended follow-up period. Although previously reported *TS* and *ERCC1* tend to be associated with poor prognosis of our patients, the association was not significant enough for them to be considered for our predictive model ($P=0.073$ and 0.076 , for *TS* and *ERCC1*, respectively). Notably, the outcome discrimination predicted by the classifier was statistically significant on two validation groups, including the only available published microarray data set from chemotherapy-treated gastric cancer patients.⁴ Although the sample size of our validation set is relatively small, it is nonetheless large enough to show that our three-gene predictor provides a statistically significant discrimination of patient outcome in multivariate survival analyses. The study design we employed is consistent with an allocation of two-third to one-third training-to-test allocation as recommended by statisticians.²⁵

We combined analyses of gene expression changes identified by expression profiling with the identification of DNA copy number changes using array CGH to develop a predictor composed of a much smaller number of critical genes that potentially could be of clinical utility. We identified *MYC*, *EGFR* and *FGFR2* in regions of amplification, as well as in the gene expression signature related to clinical outcome after CF therapy, suggesting that these genes might be functionally involved in determining resistance. Amplification of *MYC*, *EGFR* and *FGFR2* have previously been observed in gastric cancer at frequencies 4.8–15.5%,²⁶ 2.3–13.3%²⁷ and 3–10%,^{26,28} respectively, suggesting that, in some cases, tumors amplify these regions for selective advantage. Combined expression of these three genes could predict overall survival and time to progression of CF-treated gastric cancer patients. Thus, combining array CGH analysis with relevant transcriptional changes is a feasible approach for building a predictive model using functionally important genes and reducing the likelihood of false biomarker discovery. Transcriptional levels of genes other than *MYC*, *EGFR* and *FGFR2* identified in the amplified genomic loci were not associated with the survival of the 96 training set patients (for example, $P=0.313$ for *ERBB2*).

Primary gastric tumors are not easily measurable by current radiographic techniques, and often there are no metastatic lesions that are readily quantifiable in metastatic gastric cancer patients. To develop a predictor from the general population of gastric cancer patients in an unbiased way, this study was designed to correlate gene expression profiling of the tumors with overall survival and time to progression, not radiographic response. Overall survival is the ultimate measure of the treatment benefit afforded to a patient and is a particularly appropriate gauge for patients with metastatic gastric cancer, as radiographic assessment is problematic in such patients. The fact that both the time to progression as well as overall survival are predicted by our three-gene predictor in CF-treated patients, but not surgically treated patients, suggests that the three-gene predictor is a predictive indicator for the clinical benefit from CF.

Although *EGFR* and *FGFR2* expression have been reported to have prognostic value for gastric cancer patients treated surgically,^{29,30} we did not find the three-gene predictive index to be prognostic for surgically treated patients with gastric cancer. Our findings are consistent with previously reported experimental data on chemoresistance. Inhibitors of *EGFR* act synergistically with cisplatin³¹ and fluorouracil,³² whereas an *FGFR2* inhibitor is synergistic with fluorouracil.³³ *MYC* has been linked to cisplatin resistance in several *in vitro* models.^{34–37}

Taken together, combined expression of *MYC*, *EGFR* and *FGFR2* is predictive of poor survival in CF-treated metastatic gastric cancer patients. More focused prospective trials that are designed to test the clinical utility of this three-gene predictor are warranted.

Conflict of interest

The authors declare no conflict of interest.

Acknowledgments

The work was supported in part by National Institute of Health Intramural Program, Center for Cancer Research, National Cancer Institute, Korean National Cancer Center Grant 0910570 and Converging Research Center Program through the Ministry of Education, Science and Technology of Korea (2010K001121). We thank Dr Richard Simon for valuable discussions and critical reading of the manuscript, Dr Lyuba Varticovski for critical review of the manuscript and Dr Chang-Hee Kim, Ms Susie Korolevich, Ms Eunbyul Lee, Ms Eugene Kim and Ms Ilji Jeon for technical help.

Transcript Profiling

All expression microarray data is available at Gene Expression Omnibus (accession number GSE14210; <http://www.ncbi.nlm.nih.gov/geo>).

References

- 1 Uchida K, Danenberg PV, Danenberg KD, Grem JL. Thymidylate synthase, dihydropyrimidine dehydrogenase, ERCC1, and thymidine phosphorylase gene expression in primary and metastatic gastro-

- intestinal adenocarcinoma tissue in patients treated on a phase I trial of oxaliplatin and capecitabine. *BMC Cancer* 2008; 8: 386.
2. Ghadimi BM, Grade M, Difilippantonio MJ, Varma S, Simon R, Montagna C et al. Effectiveness of gene expression profiling for response prediction of rectal adenocarcinomas to preoperative chemoradiotherapy. *J Clin Oncol* 2005; 23: 1826–1838.
3. Rimkus C, Friederichs J, Boulesteix AL, Theisen J, Mages J, Becker K et al. Microarray-based prediction of tumor response to neoadjuvant radiochemotherapy of patients with locally advanced rectal cancer. *Clin Gastroenterol Hepatol* 2008; 6: 53–61.
4. Yamada Y, Arai T, Gotoda T, Taniguchi H, Oda I, Shiraok K et al. Identification of prognostic biomarkers in gastric cancer using endoscopic biopsy samples. *Cancer Sci* 2008; 99: 2193–2199.
5. Allen WL, Coyle VM, Jithesh PV, Protuski I, Stevenson L, Fenning C et al. Clinical determinants of response to irinotecan-based therapy derived from cell line models. *Clin Cancer Res* 2008; 14: 6647–6655.
6. Simon R, Radmacher MD, Dobbin K. Design of studies using DNA microarrays. *Genet Epidemiol* 2002; 23: 21–36.
7. Kang Y, Kang WK, Shin DB, Chen J, Xiong J, Wang J et al. Randomized phase III trial of capecitabine/cisplatin vs continuous infusion of 5-FU/cisplatin as first-line therapy in patients with advanced gastric cancer: efficacy and safety results. *J Clin Oncol* 2006; 24 (Suppl): 18s (abstr 4018).
8. Kim HK, Choi JJ, Kim HS, Kim JH, Kim E, Park IS et al. DNA microarray analysis of the correlation between gene expression patterns and acquired resistance to 5-FU/cisplatin in gastric cancer. *Biochem Biophys Res Commun* 2004; 316: 781–789.
9. Simon R, Lam A, Li MC, Ngan M, Menendez S, Zhao Y. Analysis of gene expression data using BRB-Array Tools. *Cancer Informatics* 2007; 2: 11–17.
10. Bai F, Tibshirani R. Semi-supervised methods to predict patient survival from gene expression data. *PLoS Biol* 2004; 2: E108.
11. Leung SW, Chen X, Chu KM, Yuen ST, Matly J, Ji J et al. Phospholipase A2 group IIA expression in gastric adenocarcinoma is associated with prolonged survival and less frequent metastasis. *Proc Natl Acad Sci USA* 2002; 99: 16203–16208.
12. Troyanskaya O, Cantor M, Sherlock G, Brown P, Hastie T, Tibshirani R et al. Missing value estimation methods for DNA microarrays. *Bioinformatics* 2001; 17: 520–525.
13. Weaver DA, Crawford EL, Warner KA, Elkhaiir F, Khuder SA, Willey JC. ABCCS, ERCC2, XPA and XRCC1 transcript abundance levels correlate with cisplatin chemoresistance in non-small cell lung cancer cell lines. *Mol Cancer* 2005; 4: 18–25.
14. Chiang YY, Chen SL, Hsiao YT, Huang CH, Lin TY, Chiang IP et al. Nuclear expression of dynamin-related protein 1 in lung adenocarcinomas. *Mod Pathol* 2009; 22: 1139–1150.
15. Taniguchi T, Tischkowitz M, Ameznane N, Hodgson SV, Mathew CG, Joenje H et al. Disruption of the Fanconi anemia–BRCA pathway in cisplatin-sensitive ovarian tumors. *Nat Med* 2003; 9: 568–574.
16. Guo QM, Malek RL, Kim S, Chiao C, He M, Ruffly M et al. Identification of c-myc responsive genes using rat cDNA microarray. *Cancer Res* 2000; 60: 5922–5928.
17. Balgo JM, Black EP. A gene expression predictor of response to EGFR-targeted therapy stratifies progression-free survival to cetuximab in KRAS wild-type metastatic colorectal cancer. *BMC Cancer* 2009; 9: 145–154.
18. Park SR, Chun JH, Yu MS, Lee JH, Ryu KW, Choi JJ et al. Phase II study of docetaxel and irinotecan combination chemotherapy in metastatic gastric carcinoma. *Br J Cancer* 2006; 94: 1402–1406.
19. Park SR, Chun JH, Yu MS, Lee JH, Ryu KW, Choi JJ et al. Phase II study of low-dose docetaxel/fluorouracil/cisplatin in metastatic gastric carcinoma. *Am J Clin Oncol* 2005; 28: 433–438.
20. Cunningham D, Rao S, Starling N, Iveson T, Nicolson M, Coxon F et al. Randomised multicentre phase III study comparing capecitabine with fluorouracil and oxaliplatin with cisplatin in patients with advanced oesophagogastric (OG) cancer: The REAL 2 trial. *J Clin Oncol* 2006; 24: 18s (abstr. 4017).
21. Pyrhönen S, Kuitunen T, Nyandoto P, Kouri M. Randomised comparison of fluorouracil, epidoxorubicin and methotrexate (FEMTX) plus supportive care with supportive care alone in patients with non-resectable gastric cancer. *Br J Cancer* 1995; 71: 587–591.
22. Tetzlaff ED, Cen P, Ajani JA. Emerging drugs in the treatment of advanced gastric cancer. *Expert Opin Emerg Drugs* 2008; 13: 135–144.
23. Lenz HJ, Leichman CG, Danenberg KD, Danenberg PV, Groshen S, Cohen H et al. Thymidylate synthase mRNA level in adenocarcinoma of the stomach: a predictor for primary tumor response and overall survival. *J Clin Oncol* 1996; 14: 176–182.
24. Metzger R, Leichman CG, Danenberg KD, Danenberg PV, Lenz HJ, Hayashi K et al. ERCC1 mRNA levels complement thymidylate synthase mRNA levels in predicting response and survival for gastric cancer patients receiving combination cisplatin and fluorouracil chemotherapy. *J Clin Oncol* 1998; 16: 309–316.
25. Dobbin KK, Simon RM. Optimally splitting cases for training and testing high dimensional classifiers (submitted for publication) <http://linus.nci.nih.gov/~brb/reprints.htm>.
26. Hara T, Ooi A, Kobayashi M, Mai M, Yanagihara K, Nakanishi I. Amplification of c-myc, K-sam, and c-met in gastric cancers: detection by fluorescence in situ hybridization. *Lab Invest* 1998; 78: 1143–1153.
27. Moutinho C, Mateus AR, Milanezi F, Carneiro F, Seruca R, Suriano G. Epidermal growth factor receptor structural alterations in gastric cancer. *BMC Cancer* 2008; 8: 10–15.
28. Yoshida T, Sakamoto H, Terada M. Amplified genes in cancer in upper digestive tract. *Semin Cancer Biol* 1993; 4: 33–40.
29. Lieto E, Ferraccio F, Orditura M, Castellano P, Mura AL, Pinto M et al. Expression of vascular endothelial growth factor (VEGF) and epidermal growth factor receptor (EGFR) is an independent prognostic indicator of worse outcome in gastric cancer patients. *Ann Surg Oncol* 2008; 15: 69–79.
30. Yasui W, Que NJ, Ung PP, Matsumura S, Shutoh M, Nakayama H. Molecular-pathological prognostic factors of gastric cancer: a review. *Gastric Cancer* 2005; 8: 86–94.
31. Fan Z, Baselga J, Masui H, Mendelsohn J. Antitumor effect of anti-epidermal growth factor receptor monoclonal antibodies plus cis-diamminedichloroplatinum on well established A431 cell xenografts. *Cancer Res* 1993; 53: 4637–4642.
32. Hiraishi Y, Wada T, Nakatani K, Uchida J, Iwasa T, Yoshida T et al. Synergistic antitumor effect of 5-1 and the epidermal growth factor receptor inhibitor gefitinib in non-small cell lung cancer cell lines: role of gefitinib-induced down-regulation of thymidylate synthase. *Mol Cancer Ther* 2008; 7: 599–606.
33. Yashiro M, Shinto O, Nakamura K, Tendo M, Matsuoka T, Matsuzaki T et al. Synergistic anti-tumor effects of EGFR2 inhibitor with 5-fluorouracil on scirrhous gastric carcinoma. *Int J Cancer* 2010; 126: 1004–1016.
34. Leonetti C, Bircio A, Candillaro A, Citro G, Fornari C, Mottolose M et al. Increase of cisplatin sensitivity by c-myc antisense oligodeoxynucleotides in a human metastatic melanoma inherently resistant to cisplatin. *Clin Cancer Res* 1999; 5: 2588–2595.
35. Xie XK, Yang DS, Ye ZM, Tao HM. Recombinant antisense c-myc adenovirus increase *in vitro* sensitivity of osteosarcoma MG-63 cells to cisplatin. *Cancer Invest* 2006; 24: 1–8.
36. Knapp DC, Mata JE, Reddy MT, Devi GR, Iversen PL. Resistance to chemotherapeutic drugs overcome by c-Myc inhibition in a Lewis lung carcinoma murine model. *Anticancer Drugs* 2003; 14: 39–47.
37. Bircio A, Benassi B, Fiorentino F, Zupi G. Glutathione depletion induced by c-Myc downregulation triggers apoptosis on treatment with alkylating agents. *Neoplasia* 2004; 6: 195–206.



This work is licensed under the Creative Commons Attribution-NonCommercial-NoDerivative Works 3.0 Unported License. To view a copy of this license, visit <http://creativecommons.org/licenses/by-nc-nd/3.0/>

Supplementary Information accompanies the paper on the www.nature.com/tpj

The Pharmacogenomics Journal website (<http://www.nature.com/tpj>)

